

MIAPH-PP-67.8

Plasma Physics Bulletin  
Vol. 7 No. 1 November 1967

## FIELD EMISSION OF CESIUM IONS\*

by

Nicholas Sama\*\*

Department of Physics  
University of Miami  
Coral Gables, Florida

## ABSTRACT

The field emission of cesium ions from a positive electrode is formulated for the range of electric field over which an image potential binds the ions to the electrode surface.

Recent investigations on the ionization of gas atoms by a metal surface are utilized, in conjunction with steady-state arguments, to yield an expression for the ion supply at the electrode surface. A tunnelling process in the presence of an electric field is then considered, and the ion emission obtained in terms of fundamental constants and pertinent parameters.

As part of the overall problem, the effect on the emission current of fractional adsorbed atomic layers on the electrode is examined; not surprisingly, the non-uniform properties of a real electrode lead to the same difficulties in the description of ion emission as those met in the case of electron field emission.

\* Supported by NASA Research Grant NsG-62/10-007-003,  
Harry S. Robertson, Principal Investigator

\*\* Supported by NASA Graduate Fellowship

## I. INTRODUCTION

The field emission of ions from an electrode has important consequences for discharge-produced plasmas operating at relatively low temperatures ( $T \lesssim 800^\circ\text{K}$ ). It plays a key role in determining, among other things, the potential function in the electrode vicinity.

The present investigation is directed towards a formulation of field ion emission for that range of electric field wherein an image-force well binds the ions to the electrode surface. This is the range normally encountered in plasmas produced by a gaseous discharge, and information about the ion current field-emitted into the plasma will give some insight into the anode-plasma accommodation necessary for stable operation.

With very high electric fields ( $10^{10}$  v/m and above), the image potential well of an ion in the vicinity of a metal electrode is completely collapsed. For this situation, the emission proceeds under conditions very different from those considered here. The emission for the very high field range has been investigated by Good and Müller<sup>1</sup>, among others, in connection with desorption techniques and Field Ion Microscope studies.

The general approach to the present problem will be as follows:

1. The anode surface will be considered as a featureless,

two-dimensional continuum, with an ion supply available thereat via a surface ionization process by which neutral adsorbed atoms lose a valence electron to the metal through a tunnelling effect. The resulting ion is bound in a combination image and van der Waals potential well, with the latter supplying a strong close-range repulsion effect. Since the surface ionization process cannot go on indefinitely, equilibrium and steady-state arguments are utilized to give the surface ion number density. The expression resulting from the steady-state situation is then used as a starting point in obtaining the ion supply function.

2. If an electric field exists at the anode surface and vicinity such that the anode is positive with respect to the plasma, then the ion potential well is modified so that it is finite, with a barrier forming between well and plasma.

3. A tunnelling process is then considered by which the ions are emitted into the plasma, this emission being formulated in terms of the surface field, ion species, temperature, etc.

The problem is thus very similar to that of electron field emission, except that some important modifications arise in the ion supply function and in the tunnelling process. For the case of ion emission, energies up to the barrier top must be considered, whereas the electron field emission process can<sup>1</sup> conveniently be terminated in the neighborhood of the metal fermi level.

The specific case of a tungsten anode with cesium vapor as

the discharge medium will be considered throughout. The discussion is fairly general, however, and such modifications as may be required for extension to other situations should not be of a major nature, especially for the heavier alkali metal vapors as discharge media.

It is important to point out that for ordinary emission densities, the present lack of a rigorously valid surface ionization rate expression does not significantly impair the validity of the results here obtained. This is discussed more fully in Sec.VI, where it is pointed out that over the range of emission densities normally encountered, the emission equation is quite insensitive to the details of the ionization rate. Some physical considerations that support this result, and in fact require it, are also presented there.

In Secs.II and III, the model on which the ion supply function is based is presented. In Sec.IV, a brief statement is made regarding the well-known formulation of the emission process in terms of a "supply function" and "transmission coefficient", and the rest of the section is then devoted to obtaining the supply function. Section V gives the transmission coefficient, and this is combined in Sec.VI with the result of Sec.IV to obtain the emission current. In Sec.VII, the observed<sup>2</sup> dependence of the electrode work function on the adsorbed neutral atom fraction is considered, and the emission equation then discussed in Sec.VIII.

## II. EQUILIBRIUM ION DENSITY ON ANODE SURFACE

Consider first a plane, cold, metal electrode with no applied electric field. The energetics involved when a neutral atom approaches the anode (treated here as an idealized, structureless plane) can be represented as in Fig. 1. This diagram shows the potential energy scheme for the valence electron of the neutral atom as modified by the image forces present in the vicinity of the anode.

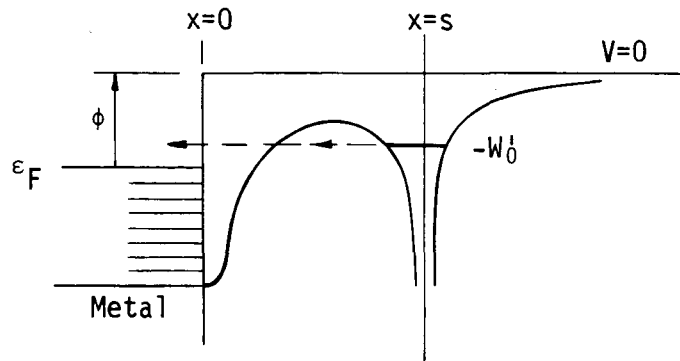


Fig.1. Potential energy of valence electron near metal.

In Fig.1,  $x$  denotes the distance along the normal to the surface, with the zero of energy taken as that of a point distant from both electrode and atom core. The fermi level  $\epsilon_F$  for the metal is measured from the bottom of the conduction band, and  $\phi$  is the metal work function. The level  $-W_0'$  is the perturbed ground state energy of the valence electron below the  $V = 0$  reference, with

$W_0^1 > 0$ . The valence level is shifted<sup>3</sup> at small distances from the electrode by the surface interaction. Due to the probability of the transition of the valence electron into the metal (see below), the level is also broadened. This is not shown in Fig.1 and in subsequent figures for the sake of clarity.

If  $\phi > W_0^1$  for a particular combination of metal and neutral atom, then the transition of the valence electron into the metal indicated in Fig.1 may take place, leading to ionization of the neutral atom by the metal surface. The theory of this process has recently been discussed by Boudreaux and Cutler<sup>4,5</sup>, and by Gadzuk<sup>6</sup>, who considers the specific case of cesium on tungsten. Experimentally, the production of ions at a metal surface was observed many years ago. Taylor and Langmuir<sup>2</sup> give an excellent account of this.

The above process clearly cannot continue indefinitely, so that some mechanism must exist that limits the production of ions at the surface. Otherwise, a metallic electrode would eventually remove all gas atoms from the surrounding space, since the surface ions would be bound by an image potential, and successive adsorptions and ionizations of the gas atoms outside the electrode would in time result in their all being firmly bound to the electrode in the ionic state.

An obvious limiting mechanism is available in the form of backward transitions, i.e., the neutralization of surface-bound

ions by electrons tunnelling from the metal. This sort of process has been extensively studied by Hagstrum<sup>7-10</sup>.

Much more recently, Gadzuk<sup>3</sup>, in a second calculation towards obtaining the ionization rate, makes the detailed-balance assumption that the ionization and neutralization rates must be equal. This must be true eventually (for no ion current), but when, and under what conditions? He unfortunately does not elaborate on this point, and so one of the objectives of the present investigation is to obtain an estimate of the conditions necessary for the equality of the ionization and neutralization rates. It will be seen that a method for obtaining the surface ion density emerges from the analysis.

The difficulty with most of the published investigations on both ionization and neutralization transition rates is that they have so far been considered completely out of context, with no concern for the effects and/or demands of associated circuitry and local surface conditions. Thus, for example, the neutralization rate must of necessity depend on the ion density on the electrode surface, with an obviously zero rate for zero ion density. But if neutralization requires a non-zero surface ion density, the effect of such a density on the neutralization energetics must be taken into account. So far, this has not been done, so that extant calculations cannot be quite correct. Still another effect that has been neglected but which is significant is

as follows: Whenever the neutral atom is ionized on the surface, there must necessarily occur a "switch" in potential for the resulting ion. That is, the ion now finds itself in a combination adsorption and image potential well that is much deeper ( $\sim 1$  eV) than the purely adsorption well that bound the neutral atom. Thus a surface ionization process is not describable by simply considering only the valence electron energetics; the energetics of all particles taking part in the transition must be taken into account. Otherwise, the very considerable energy associated with the switch in potentials simply vanishes (or is created). The following two processes are likely possibilities in the ionization transition:

1. The neutral atom is ionized, with the tunnelling electron carrying away only the energy difference between the valence level and the metal level it occupies after the transition. The resulting ion, which must now be considered as left in excited states in the adsorption and image well, subsequently decays to the lower levels via radiative or other transitions; the most likely among the latter is probably the non-radiative transfer of energy and momentum to the electrode crystal lattice.

2. The ionization is a single-stage process in which the tunnelling electron carries away the energy in (1) above and in addition that available from the switch in potentials. In any case, the tunnelling electron must decay to lower levels in the



metal by phonon de-excitation, or by other processes.

Thus the backward transition is ordinarily not as likely as the forward, or ionization transition. For if neutralization is to occur, not only must the neutralizing metal electron have sufficient energy to occupy the valence level, but in addition must supply about 1 ev to "lift" the ion up to the adsorption well, e.g., if the unoccupied valence level is at the same energy as the metal fermi level, only electrons from about 1 ev above  $\epsilon_F$  can bring about neutralization. At ordinary temperatures, the population of metal electrons at this level may be too small to produce a significant neutralization rate. However, consider the following: If field conditions at the electrode surface are such that a potential barrier exists for the ions, then it turns out (see below) that the resulting ion (i.e., charge) accumulation will modify the transition energetics such that the ionization rate decreases. At the same time, this ion accumulation renders the neutralization transitions more numerous in two ways: (1) more ions are present. (2) the energy requirements are reduced, so that the number of metal electrons energetically capable of neutralizing is increased. Thus the increase in ion surface density leads to an increasing neutralization rate on the one hand, and a decreasing ionization rate on the other. Eventually, the two must become equal, as Gadzuk assumes, but only if no ion current is being drawn from the surface. If the ion

current is non-zero (and this would seem to be the only case of practical interest), then Gadzuk's assumption cannot be quite valid. For where would the ion current come from if there were not a net surface ionization rate i.e., a departure from detail balance? Such a departure is necessary, therefore, for the attainment of ordinary steady-state conditions.

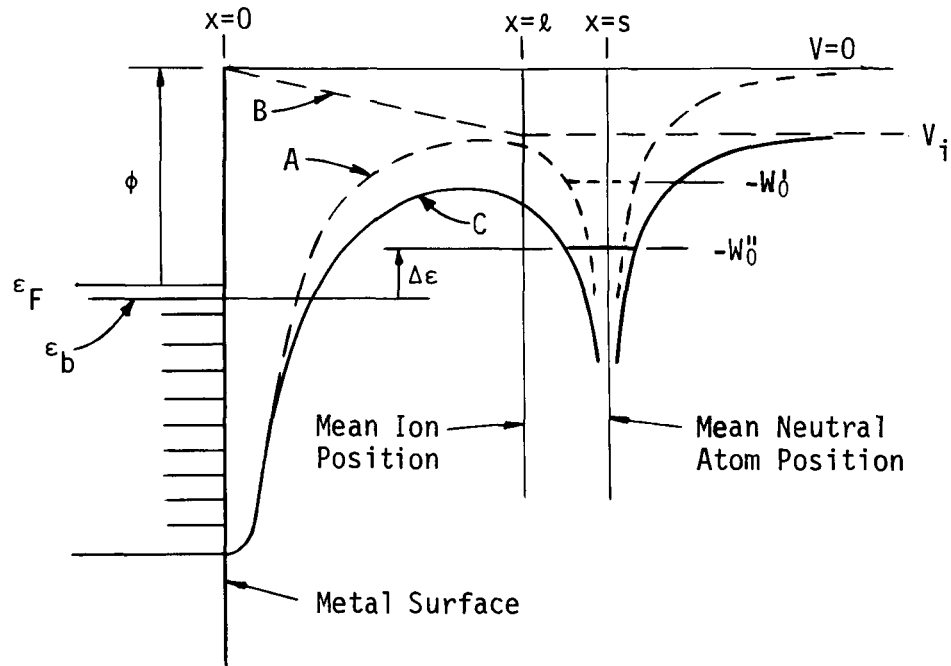
In this section, the equilibrium situation (no ion current) will be examined; here detailed balance must occur at some point, leading to an effective "termination" of ionization.

It would be desirable, of course, to have definite criteria available for when detailed balance must occur, but these do not presently exist. However, the existing surface ionization studies, and especially those of Boudreaux and Cutler<sup>5</sup>, indicate that net ionization will cease when the valence electron is at approximately the same energy as the metal fermi level. Most of the surface ionization studies require this result for any reasonable correspondence between theory and experiment, and so it will be assumed that there is some energy  $\epsilon_b$  in the neighborhood of  $\epsilon_F$  (see Fig.2), that defines the valence electron energy at which net ionization ceases. The results of Boudreaux and Cutler indicate that  $|\epsilon_F - \epsilon_b|$  must be very small (less than 0.1 ev) if their findings are to correspond with experiment. At any rate, it turns out that the precise value of  $\epsilon_b$  is of no great importance (see Sec.III) provided that  $\epsilon_F - \epsilon_b \leq 0.5$  ev, and so  $\epsilon_b$  is

shown in Fig.2 with the understanding that it is in the range 0 - 0.5 eV below  $\epsilon_F$ . In the light of the foregoing discussion, consider then the following.

Under equilibrium conditions, the ions, because of their surface mobility, can be regarded over a time interval as being continuously distributed over the surface and at an average distance  $\lambda$  from it. Hence they can be adequately represented by a sheet of uniform density at a distance  $\lambda$  from the electrode surface. The adsorbed neutral atoms will likewise appear as a sheet at some distance  $s$  from the surface, but more or less localized about the lattice adsorption sites. This localization, however, is of no real importance for the present calculation.

A question which arises is whether the mean distance  $\lambda$  of the ions is greater or less than the mean distance  $s$  of the neutral atoms. This is not easily answered at the present time because of the scant knowledge of the potentials involved at small distances from the electrode. Fortunately, the choice of one or the other of the two possibilities leads only to minor numerical modifications and does not enter into the essence of the calculation. The choice  $\lambda < s$  will be made as the more likely, leading to a potential energy diagram for an adsorbed neutral atom as in Fig.2. The same convention is used as for Fig.1. Curve A is the potential energy of the valence electron in the absence of the ion sheet. The perturbed valence electron level is  $-W'_0$  as before.



Note:  $-W''$  is measured from  $V_i = -\sigma e^2 x / \epsilon_0$ .

Fig.2. Potential energy of valence electron in presence of ion sheet.

Curve B is the potential energy contribution due to the ion sheet of number density  $\sigma$ ; it is given in MKS units by  $-\sigma e^2 x / \epsilon_0$  for  $x \leq l$  and has the constant value  $-\sigma e^2 l / \epsilon_0$  for  $x \geq l$ . This of course is not realistic; because of the ions' motion in their own well, the potential energy will actually drop off more or less slowly, depending on the ion temperature. However, this introduces no important changes in the calculation. Finally, curve C represents the potential energy due to A and B. Because of the ion sheet, the valence level is again shifted; it is denoted by

$-W_0''$  and is now measured from the new reference  $V_j = \sigma e^2 \ell / \epsilon_0$ . The energy  $\Delta\epsilon$  is that of the valence electron above the level  $\epsilon_b$ , mentioned earlier, that defines the reference valence level at which net ionization ceases.

It is clear from Fig.2 that if net ionization requires  $\Delta\epsilon > 0$ , then detailed balance must occur when  $\sigma e^2 \ell / \epsilon_0 + W_0'' = \phi + \epsilon_F - \epsilon_b$ , whence

$$\sigma = (\epsilon_0 / e^2 \ell) [\phi - W_0'' + \epsilon_F - \epsilon_b] \quad (1)$$

gives the equilibrium ion number density. As an illustration of Eq.(1), the case of cesium on tungsten may be considered. There is a slight difficulty in that the value of  $W_0''$  has not been calculated. However, for illustrational purposes, the value of  $W_0'$  (3.6 eV) calculated by Gadzuk may be used. The result will not be affected by very much (see Sec.VII). For tungsten,  $\phi = 4.6$  eV; using  $\ell = 4 \text{ \AA}$  and  $\epsilon_b \approx \epsilon_F$ ,  $\sigma \approx 1.38 \times 10^{13} \text{ cm}^{-2}$  is obtained from Eq.(1). In terms of Langmuir's determination of  $4.8 \times 10^{14} \text{ cm}^{-2}$  as a monolayer of neutral cesium on tungsten, this is about 2.8% of a monolayer (though the term does not apply for ions; it is used only for comparison purposes).

In the above, the effect of thermal ion emission over the barrier top has been neglected; for zero applied field, the ion potential barrier is infinite, so that only ions with  $W > 0$  can contribute to the current. However, the number of ions with

$W > 0$  will be negligibly small at ordinary temperatures relative to those with  $W < 0$ . Hence they need not be considered.

A fortunate consequence of Eq.(1) is that the mean spacing between ions (on the order of  $10^{-6}$  cm) will be a good deal larger than the average distance of the ions from the surface. Because of this, it will be possible when considering ion tunnelling in Sec.V to include only the image and applied fields, with ion-ion interactions as small and for the present time negligible. Moreover, as current is drawn from the ion reservoir on the surface, the steady-state ion surface density decreases from the equilibrium value. The steady-state value of  $\sigma$  can be computed by use of the results of Secs.III and VI; for ordinary emission densities,  $\sigma$  is well below  $10^{13}$  cm<sup>-2</sup>.

### III. STEADY STATE ION DENSITY WITH CURRENT BEING DRAWN

With an applied electric field, two effects will occur:

(a) The applied field further modifies the potential energy scheme of Fig.2 for the valence electron of the neutral atom.

(b) The potential energy well of whatever ions may be present, which binds them to the surface, is also modified and an ion current will be drawn from the surface ion supply produced by the surface ionization process.

The effect (b) will be considered later in connection with the emission current. The effect of (a) is to contribute a potential energy  $V_F = eEx$  to the valence electron potential energy, Fig.2. An additional level shift for the valence electron is to be expected; the new level will be denoted  $-W_0'''$ . A simplified potential energy diagram, Fig.3, shows the potential energy due to all the sources discussed.

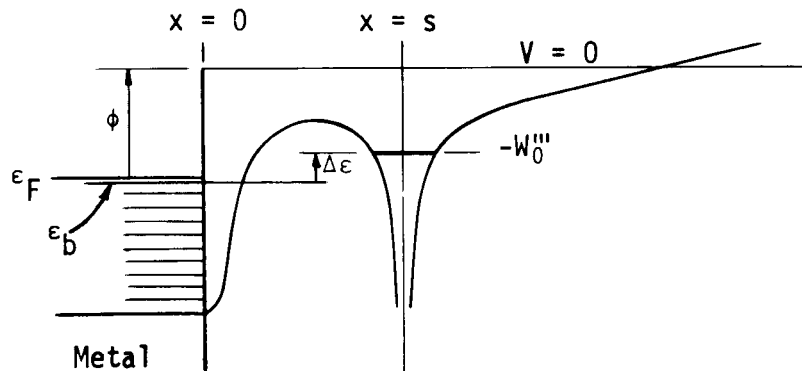


Fig.3. Modified valence electron potential energy.

The energy  $\Delta\varepsilon$  of the valence electron above the reference level  $\varepsilon_b$  can be expressed in terms of the mean quantities  $\ell$  and  $s$  by

$$\Delta\varepsilon = \phi + (\varepsilon_F - \varepsilon_b) - [W_0^0 + \sigma e^2 \ell / \varepsilon_0 - eEs] \quad (2)$$

where  $\ell$ ,  $s$ , are the mean ion and neutral atom positions, respectively. If now the transition rate  $w(\Delta\varepsilon)$  for neutral  $\rightarrow$  ion on the surface is known as a function of  $\Delta\varepsilon$ , and if the adsorbed neutral atom density is  $\sigma_0$ , then in the steady state with a current density  $j$  being drawn, it is necessary that

$$j = e\sigma_0 w(\Delta\varepsilon). \quad (3)$$

Equation (3) is generally valid if  $\sigma_0$  is the steady-state value of the adsorbed neutral atom density. However, it will be seen later (Sec.VI) that  $j$  is very small under practically all conditions, so that  $\sigma_0$  will usually not differ significantly from its equilibrium value at  $j = 0$ . Thus  $\sigma_0$  will be considered as known from an appropriate adsorption isotherm and treated as constant over the range of  $j$  which is of interest here.

An expression for the transition rate  $w(\Delta\varepsilon)$  which is completely satisfactory is not yet available. The result of Boudreaux and Cutler<sup>4,5</sup> appears to be reasonably derived, but the necessary cut-off in ionization at  $\Delta\varepsilon = 0$  does not appear explicitly in their rate equation, as it actually should. Presumably, what



they have done is to include a cutoff at the fermi level as an ad hoc addendum to their calculation, but they do not elaborate on this important point. Also, they are concerned mainly with a neutral atom approaching the electrode surface, rather than adsorbed thereon. No significant modification should be introduced by this detail, however.

Gadzuk's calculation<sup>6</sup> is framed in the same way as those of Boudreaux and Cutler, except that he considers the neutral atom as adsorbed on the electrode surface. There are unfortunately some uncertainties about the details of his derivation. Among other things, his result is incredibly high: For  $\Delta\varepsilon \approx 1$  ev, a transition rate of about  $10^{15}$  sec<sup>-1</sup> is obtained. Thus even with the inclusion of a cutoff function for energies close to the fermi level, the resulting rate would require enormous currents (see Eq.(3)) for steady-state. Furthermore, he does not consider the energetics involved when the neutral atom transits, as outlined in Sec.II, from the adsorption potential just prior to ionization to the image potential just after.

In view of the uncertainty here felt about the published rate expressions, the theory of surface ionization utilized by the above investigators will be briefly presented, and then an expression for the ionization rate usable here will be discussed. Essentially, this will mean representing the transition rate by a first order approximation in  $\Delta\varepsilon$ .

Typically<sup>4,5,6</sup>, the ionization rate is given to first order by

$$w = (2\pi/\hbar)N(\epsilon_f)|\langle \psi_f|V_p|\psi_i \rangle|^2, \quad (4)$$

where  $\epsilon_f = \epsilon_b + \Delta\epsilon = \epsilon_i$  is the energy of the valence electron above the bottom of the metal conduction band.  $N(\epsilon_f)$  is the density of final electron states and is given by  $N(\epsilon_f) = \text{const} \times \sqrt{\epsilon_f}$ ;  $V_p$  is the perturbing potential (considered as due to surface forces). The states  $\psi_i, \psi_f$  are the initial and final electron states, respectively, and  $|\langle \psi_f|V_p|\psi_i \rangle|^2$  is the matrix element for the transition. Denoting the matrix element and constants appearing in Eq.(4) by  $A'$ , one can write  $w(\Delta\epsilon) = A'(\epsilon_b + \Delta\epsilon)^{1/2}$ . But by the definition of  $\epsilon_b$ , it is necessary that  $w(0) = 0$ , and so the factor  $A'$  must have an expansion of the form

$$A' = A''\Delta\epsilon + A'''(\Delta\epsilon)^2 + \dots$$

where, for  $\Delta\epsilon$  small enough,  $A' \approx A''\Delta\epsilon$  to sufficient accuracy. It will be assumed here, and this is supported in Sec.VII, that this small  $\Delta\epsilon$  approximation will be sufficiently accurate for present purposes. Thus, in this approximation,

$$w(\Delta\epsilon) \approx A''\Delta\epsilon(\epsilon_b + \Delta\epsilon)^{1/2}. \quad (5)$$

As will be seen later, the variation in  $\Delta\epsilon$  over the range of interest is such that  $\Delta\epsilon \ll \epsilon_b$ ; this is because  $\epsilon_b \approx 5$  ev, while

while  $\Delta\epsilon$ , for normal currents, is always less than a few tenths of an electron volts. Hence  $(\epsilon_b + \Delta\epsilon)$  is sensibly constant, and  $w \approx A\Delta\epsilon$  results. With a fitting such that  $w \approx 10^6 \text{ sec}^{-1}$  for  $\Delta\epsilon \approx 1 \text{ ev}$ ,  $A \approx 10^{25} \text{ sec}^{-1} \text{ joule}^{-1}$  is obtained. In Sec.VI, it will be seen that over the most interesting emission current range,  $j$  is insensitive to variation in the value of  $A$  over many orders of magnitude. Thus there is considerable latitude available in the choice of  $A$ , and reasonable results may be expected from the use of Eq.(6) below as a representation for  $w(\Delta\epsilon)$  unless the assumed linearity in  $\Delta\epsilon$  is too far off. The value of  $A$  that has been chosen here is considered, on the basis of Gadzuk's work, to be a reasonable lower bound; should the true value be larger, and this seems likely, then the approximation is improved thereby.

Finally, then

$$w(\Delta\epsilon) = A\Delta\epsilon = 10^{25}\Delta\epsilon \text{ joule}^{-1} \text{ sec}^{-1} \quad (6)$$

will be used, with  $\Delta\epsilon$  in joules.

Equations (2) and (6) in (3) give

$$j = Ae\sigma_0\Delta\epsilon = Ae\sigma_0[\phi + (\epsilon_F - \epsilon_b) - W_0'' - \sigma e^2\ell/\epsilon_0 + eEs],$$

whence the ion surface density at steady-state is

$$\sigma = (\epsilon_0/e^2\ell)[\mu + eEs - j/Ae\sigma_0], \quad (7)$$

with  $\mu = \phi + (\epsilon_F - \epsilon_b) - W_0''$ .

#### IV. THE ION SUPPLY FUNCTION

The ions produced on the electrode surface by the surface ionization process will be bound thereto by a combination image and van der Waals well of form similar to the dashed curve shown in Fig.4. Due to the lack of a firm knowledge of the potential energy for  $x$  small, a sharp cut-off at  $x = x_0 = 4\text{\AA}$  will be assumed. The sharp cut-off is justifiable because of the very large repulsive<sup>11</sup> forces that come into play for small  $x$ . The value  $x_0 = 4\text{\AA}$  is taken from adsorption data<sup>11</sup> and should be reasonably accurate. While other measurement techniques have yielded substantially different values for  $x_0$ , this value will be adopted as probably the most reliable for use here.

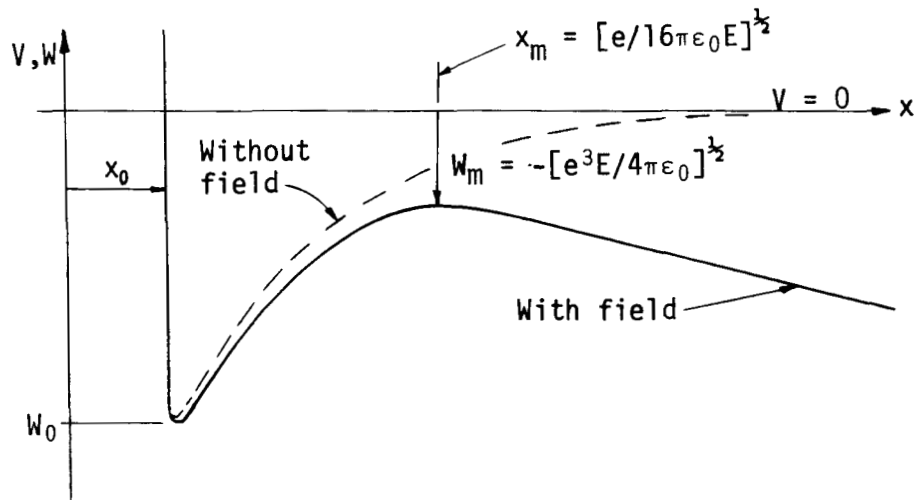


Fig. 4. Ion potential well.

The application of an electric field  $E$  directed along the

positive x-direction will lead to two emission processes:

(a) By lowering the barrier maximum of Fig.4, an enhanced thermal emission will occur.

(b) For ions with energies below  $W_m$ , emission takes place by way of a tunnelling effect. This is a strictly field emission process.

The ion emission density due to (a) will not be considered here; that due to (b) is given by

$$j = q \int_{W_0}^{W_m} N(W)T(W)dW, \quad (8)$$

where  $W_0$  = energy at bottom of potential well,  $T(W)$  = transmission coefficient,  $N(W)$  = supply function = number of ions striking barrier from left per unit time per unit area per unit energy interval, and  $q$  is the ion charge. Only singly ionized atoms will be considered, so that  $q = e$ .

$N(W)$  can be found provided: (1) the ions remain essentially in equilibrium with emission taking place, and (2) the ion statistics are known. The assumption of equilibrium used in this section will be supported by the results of Sec.VI, where the emitted current density is seen to be much smaller than the random current density. Because of the large ion mass, and also because the surface density is dilute, Boltzmann statistics apply rigorously for a system of either bosons or fermions. For example,

a system of fermions with  $\sigma = 10^{13} \text{ cm}^{-2}$  has a fermi temperature of about  $0.01^\circ\text{K}$ .

In this section,  $N(W)dW$  will be found. The next section will deal with the transmission coefficient  $T(W)$ . These are then assembled in Sec.VI according to Eq.(8) to give an expression for the emission current  $j$ .

In order to obtain  $N(W)dW$ , the ions will be considered as:

1. a three dimensional gas as far as the energetics are concerned. There are two degrees of freedom along the surface and a vibrational degree of freedom along the normal to the surface. Equipartition of energy is assumed to hold.

2. describable by a density  $\rho(x) = K\exp[-\beta V(x)]$ , where  $\beta$  is  $1/kT$ . The dimensions of  $\rho(x)$  are ions per unit area per unit  $x$ -interval. While a rigorously valid expression would be given by  $\rho(x) = K\Sigma|\psi_n(x)|^2\exp(-\beta W_n)$ , where the  $\psi_n$  are the energy eigenfunctions for the ions in the potential well, the proposed expression should be reasonably valid at the temperatures normally encountered in cesium discharges.

The quantity  $K$  in  $\rho(x)$  is a normalization factor such that  $K\int_{x_0}^{x_m}\rho(x)dx = \sigma$ . That is, the ions comprising  $\sigma$  are considered as being essentially localized in  $x_0 \leq x \leq x_m$  (see Fig.4). Thus  $K$  is given by

$$K = \sigma / \int_{x_0}^{x_m} \exp[-\beta V(x)] dx. \quad (9)$$

It was not found possible to evaluate the integral appearing in Eq.(9), so that a computer solution had to be resorted to. This integral is parametric in  $T$  and the field  $E$ , which enters via the potential  $V(x)$ ; it will henceforth be denoted by  $L(E,T)$ . The ion density function can thus be written

$$\rho(x) = (\sigma/L)e^{-\beta V(x)}, \quad (10)$$

with the expression  $L$  carried symbolically for now. The computer solution will be incorporated into the emission equation in Section VI.

Consider now the particle current density incident on the barrier of Fig.4 from the left. The contribution from ions within the momentum interval  $dp_x$  is

$$N(p_x)dp_x = \rho(x)(\beta/2\pi m)^{1/2} \exp[-\beta p_x^2/2m] (p_x/m) dp_x, \quad (11)$$

since the ions are free in the directions along the surface. Because the transmission coefficient (Sec.V) must be expressed in terms of the energy of the tunnelling ion, Eq.(11) must be rewritten in terms of the ion energy. The energy of the vibrational states is  $W = p_x^2/2m + V(x)$ . For some arbitrary fixed  $x$  in  $x_0 \leq x \leq x_m$ ,

$$dW_{(x = \text{const.})} = d[V(x) + p_x^2/2m] = (p_x/m) dp_x$$

is obtained. Hence Eq.(11) becomes, in terms of the energy,

$$\begin{aligned}
 N(p_x)dp_x &= \rho(x)\sqrt{\beta/2\pi m}\exp[-\beta p_x^2/2m]dW \\
 &= (\sigma/L)\sqrt{\beta/2\pi m}\exp(-\beta W)dW = N(W)dW.
 \end{aligned}
 \tag{12}$$

It is convenient at this point to obtain the field below which an ion potential barrier will exist. With the assumed sharp cut-off in  $V(x)$ , the barrier is completely collapsed when  $x_m = x_0$ ; setting  $V'(x) = 0$ , one obtains  $x_m = (e/16\pi\epsilon_0 E)^{1/2} = 4\overset{\circ}{\text{A}}$ . Hence denoting the collapsing field by  $E_m$ , it is found that

$$E_m = 2.25 \times 10^9 \text{ v/m.} \tag{13}$$

The reliability of this value is of course dependent on the reliability of the assumed  $x_0 = 4\overset{\circ}{\text{A}}$ , as well as on the validity of the sharp cut-off assumption. That a barrier collapse does indeed take place is quite evident from Field Ion Microscope studies<sup>1</sup>.

While  $0 \leq E \leq 2.25 \times 10^9 \text{ v/m}$  defines the field range over which a tunnelling process is relevant, a much more interesting range, for present purposes, is  $0 \leq E \leq 5 \times 10^7 \text{ v/m}$  (obtainable from Figs. 7 and 8). Over the latter range, the emission current density is insensitive to the details of the ionization rate, so that reliable results can be expected therein. Moreover, fields higher than  $5 \times 10^7 \text{ v/m}$  are not likely to be found in the anode region of discharge-produced plasmas. For these reasons, much of what follows will be restricted to  $E \leq 5 \times 10^7 \text{ v/m}$ ; the restriction,



whenever imposed, will be pointed out in the text. In view of the anode fields normally encountered, it is reasonable to state that the reduced range of  $E$  does not really amount to a restriction of any significance.

## V. THE TRANSMISSION COEFFICIENT

The transmissivity of the barrier is obtained by a modified WKB method<sup>12,13</sup> which has been shown to be valid for all energies of the incident particle, including those over the barrier top. The same functional expression results for  $T(W)$  as is obtained by the usual WKB method, but the method of derivation extends its validity to all energies.

The transmissivity is given<sup>12,13</sup> by

$$T(W) = [1 + Q(W)]^{-1}, \quad (14)$$

where

$$Q(W) = (2/\hbar) \int_{x_1}^{x_2} [2m\{V(x) - W\}]^{1/2} dx, \quad (15)$$

and  $x_1, x_2$ , are as shown in Fig.5. With  $V(x) = -e^2/16\pi\epsilon_0 x - eEx$ , Eq.(15) becomes

$$Q(W) = (2/\hbar) \int_{x_1}^{x_2} [-2m(e^2/16\pi\epsilon_0 x + eEx + W)]^{1/2} dx. \quad (16)$$

The above variables may be referred to the potential energy diagram of Fig.5. Only those values of  $W$  in  $W_0 \leq W \leq W_m$  will be considered here, so that the quantity inside the square brackets of Eq.(16) is always  $\geq 0$ . The values of  $x_1$  and  $x_2$  may be related to the energy of the tunnelling ion. They are given by  $x_1 = -(W/2eE)(1 - \sqrt{1-G})$ ,  $x_2 = -(W/2eE)(1 + \sqrt{1-G})$ , where  $G$  is

given by  $G = e^3 E / 4\pi\epsilon_0 W^2$ . Since  $W < 0$ , and  $G \leq 1$  (see Fig.5),  $x_1$  and  $x_2$  are always real and positive.

The integral in Eq.(16) has been evaluated<sup>1</sup> exactly and is given by

$$Q(W) = BE^{-1/4} y^{-3/2} v(y) = \alpha(E) y^{-3/2} v(y), \quad (17)$$

where

$$\left. \begin{aligned} \alpha(E) &= BE^{-1/4}, \\ B &= 4\sqrt{2m} a^{3/4} / 3\hbar e, \\ a &= e^3 / 4\pi\epsilon_0, \\ y &= -\sqrt{aE}/W, \\ v(y) &= (1/\sqrt{2})(1 + \sqrt{1-y^2})^{1/2} [F(k) - (1 - \sqrt{1-y^2})K(k)], \\ k^2 &= 2(1-y^2)^{1/2} / (1 + \sqrt{1-y^2}), \\ F(k) &= \int_0^{\pi/2} [1 - k^2 \sin^2 \phi]^{1/2} d\phi \\ K(k) &= \int_0^{\pi/2} [1 - k^2 \sin^2 \phi]^{-1/2} d\phi \end{aligned} \right\} (18)$$

and  $y$  ranges over  $0 \leq y \leq 1$ , corresponding to  $-\infty < W \leq W_m$ .  $W_m$  is the energy at the top of the potential energy barrier and is given by  $W_m = -[e^3 E / 4\pi\epsilon_0]^{1/2}$ .

By use Eqs. (12), (14), and (17), one can write Eq.(8) as

$$j = (e\sigma/L)(\beta/2\pi m)^{1/2} \int_{W_0}^{W_m} \frac{\exp(-W)dW}{1 + \exp[y^{-3/2}v(y)]}, \quad (19)$$

where  $y$ ,  $v(y)$  are as given by Eqs.(18).

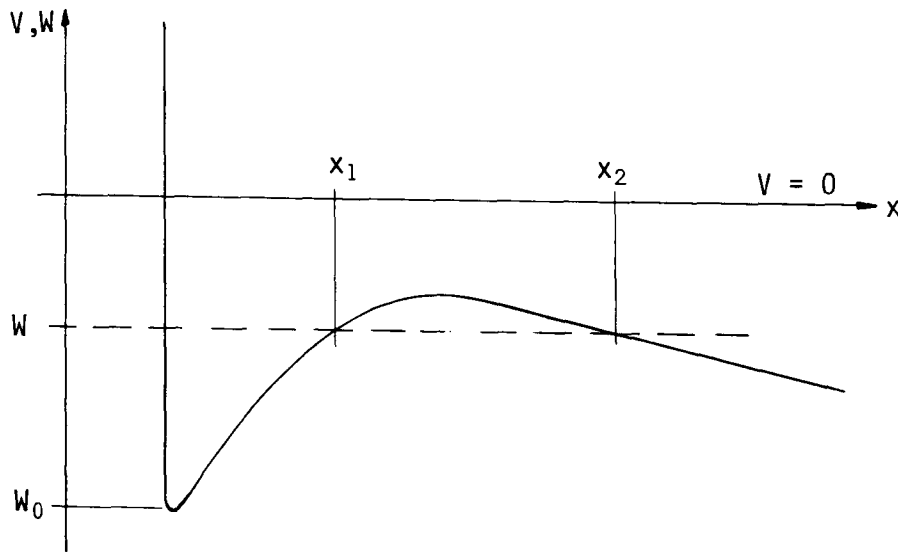


Fig. 5. Ion potential well with details relevant to tunnelling.

A glance at (18) for  $v(y)$  shows that to obtain an exact value of (19) is probably hopeless; therefore, an approximating expression for  $T(W)$  must be found.

Before proceeding, note that Eq.(19) is written in a hybrid form for now because it is easier to obtain an approximation for  $T(W)$  in terms of the quantities defined in Eqs.(18). Equation (19) can be re-expressed solely in terms of  $W$  once a reasonable approximation is obtained.

The variable  $y$ , as already noted, ranges over  $0 \leq y \leq 1$ , corresponding to  $-\infty < W \leq W_m$ . It can be seen that this range of  $W$  does not correspond to the physical situation represented by the potential energy curve of Fig.5, for there the lower limit  $W_0$  is some finite quantity. However, it is shown in Sec.6 that no significant error results from the substitution  $W_0 \rightarrow -\infty$  at the lower limit.

The details of the approximation of Eq.(17) and  $T(W)$  appear in the Appendix. The result obtained there is

$$T(W) = \frac{1}{2} \exp[-\gamma(W/W_m - 1)], \quad (20)$$

with  $\gamma(E) = \pi\alpha(E)/\sqrt{8}$ . While (20) can differ appreciably from (14) for  $W \ll W_m$ , the integral (8) will be in error by no more than a few percent because of the very rapid drop-off in the value of the integrand as  $W$  decreases. A fuller discussion may be found in the Appendix.

## VI. THE EMISSION CURRENT

By use of the expressions (12) and (20) in Eq.(8), one obtains for the emission current

$$\begin{aligned}
 j &= \frac{e\sigma}{2L} \left( \frac{\beta}{2\pi m} \right)^{\frac{1}{2}} \int_{w_0}^{w_m} e^{-\beta w} e^{\gamma(1 - w/w_m)} dw \\
 &= \frac{e\sigma}{2L} \left( \frac{\beta}{2\pi m} \right)^{\frac{1}{2}} e^{\gamma} \int_{w_0}^{w_m} e^{-(\gamma/w_m + \beta)w} dw \\
 &= \frac{e\sigma}{2L} \left( \frac{\beta}{2\pi m} \right)^{\frac{1}{2}} \frac{e^{\gamma}}{\gamma\sqrt{1/aE} - \beta} \left[ e^{\beta\sqrt{aE}-\gamma} - e^{(\beta\sqrt{aE}-\gamma)\zeta} \right], \quad (21)
 \end{aligned}$$

where  $\zeta = w_0/w_m > 1$ . Implicit in the evaluation of (21) is the assumption that the energy levels of the ions in the potential well form a continuous spectrum. This is a good approximation because the ions are very massive. A rough calculation based on adsorption data<sup>11</sup> gives a level spacing of about 0.002 eV at the bottom of the well and much smaller spacing above the neighborhood of the bottom. Moreover, the broadening of the upper levels by the finite tunnelling lifetime is at least several times the level spacing, so that a true continuum results near the barrier top; since only the topmost levels are relevant to ion emission (see immediately below), the continuous spectrum assumption can be considered to be rigorously valid.

Equation (21) can be cleaned up considerably for the following reasons: The maximum field relevant to a tunnelling process

is  $E_m = 2.25 \times 10^9$  v/m, and since the expression

$$\gamma - \beta\sqrt{aE} = 8.70 \times 10^5 E^{-\frac{1}{4}} - 0.434 T^{-1} E^{\frac{1}{2}} \quad (22)$$

is a decreasing function of  $E$ , it takes on its minimum value at  $E = E_m$ . Choosing  $T = 100^\circ\text{K}$  as an extreme possibility, there results

$$\gamma - \beta\sqrt{aE} \geq 3788. \quad (23)$$

In actual application to the case of a cesium discharge, where  $T$  is usually in the range  $400\text{-}600^\circ\text{K}$ , the lower bound of (23) will be somewhat larger, but not by very much because the first term dominates.

Using (23), one obtains the ratio of the second term to the first in the brackets of Eq.(21) as

$$R \leq e^{-3788(\zeta - 1)}. \quad (24)$$

Thus the second term is negligible if  $\zeta > \sim 1.002$ . In order to discuss the relative magnitudes of the terms in Eq.(21) on a quantitative basis, and also to prove the claims made in Sec.4 and in the Appendix about the negligibility of all contributions except those from near the barrier top, the integral (21) will be considered over regions  $R_1, R_2, R_3$  defined by

$$\begin{array}{l}
 R_1: 0.995 \leq y \leq 1.000 \\
 R_2: 0.990 \leq y \leq 0.995 \\
 R_3: 0 \leq y \leq 0.990
 \end{array}
 \left. \vphantom{\begin{array}{l} R_1 \\ R_2 \\ R_3 \end{array}} \right\} (25)$$

The variable  $y$  is  $W_m/W$  as defined in Eqs.(18). Thus  $j = \int_{W_0}^{W_m} = \int_{R_3} + \int_{R_2} + \int_{R_1} = \int_{W_0}^{W_3} + \int_{W_3}^{W_2} + \int_{W_2}^{W_m}$ , where  $W_2 = W(y = 0.995)$ ,  $W_3 = W(y = 0.990)$ ; using  $W = W_m/y$ , one obtains  $W_2 \approx 1.005W_m$ ,  $W_3 \approx 1.010W_m$ . The emission over  $R_1$  is then

$$j(R_1) = \Lambda(E, \beta) [e^{-r} - e^{-1.005r}],$$

where  $r = \gamma - \beta W_m \geq 3788$ . The second term is  $\sim 10^{-8.2}$  times the first, so that  $j(R_1) \approx \Lambda(E, \beta) e^{-r}$ . Similarly, over the region  $R_2$ ,  $j(R_2) \approx \Lambda(E, \beta) e^{-1.005r}$ . Thus  $j(R_2)/j(R_1) \approx e^{-0.005r} \approx 10^{-8.2}$ . Finally, since  $j(R_3)$  is at most  $10^2 j(R_2)$  (see Appendix), both  $j(R_2)$ ,  $j(R_3)$  can be completely neglected relative to  $j(R_1)$ . Therefore the value of Eq.(21) is essentially that given by evaluation at the upper limit only:

$$j = \frac{e\sigma}{2L} \left( \frac{\beta}{2\pi m} \right)^{1/2} \frac{e^{\beta\sqrt{aE}}}{\gamma\sqrt{1/aE} - \beta} = \frac{e\sigma}{2L} \left( \frac{\beta}{2\pi m} \right)^{1/2} \frac{e^{\beta\sqrt{aE}}}{(\pi B/\sqrt{8a})E^{-3/4} - \beta}. \quad (26)$$

The negligibility of the contributions from all levels except those near the barrier top is quite fortunate. For if this were not so, it would not be possible to skirt the present lack of knowledge of the potential near the bottom of the well. That the



contributions from all  $W \leq W_m$  can be neglected is a consequence of the large ionic mass (see Appendix).

As mentioned in Sec.IV,  $L(E,T)$  could not be obtained analytically. For this reason, plots of  $j/\sigma = \Gamma$ , the emission density per unit ion surface density, are shown in Fig.6. These plots are parametric in  $T$ . Because of the large range of  $E$  and  $\Gamma$ , it was necessary to use a log-log plot. Hence Fig.6 does not show  $\Gamma = 0$  at  $E = 0$ , but this is easily seen to be the case by examination of Eq.(26), where both  $1/L$  and the other factor in  $E$  go to zero as  $E \rightarrow 0$ .

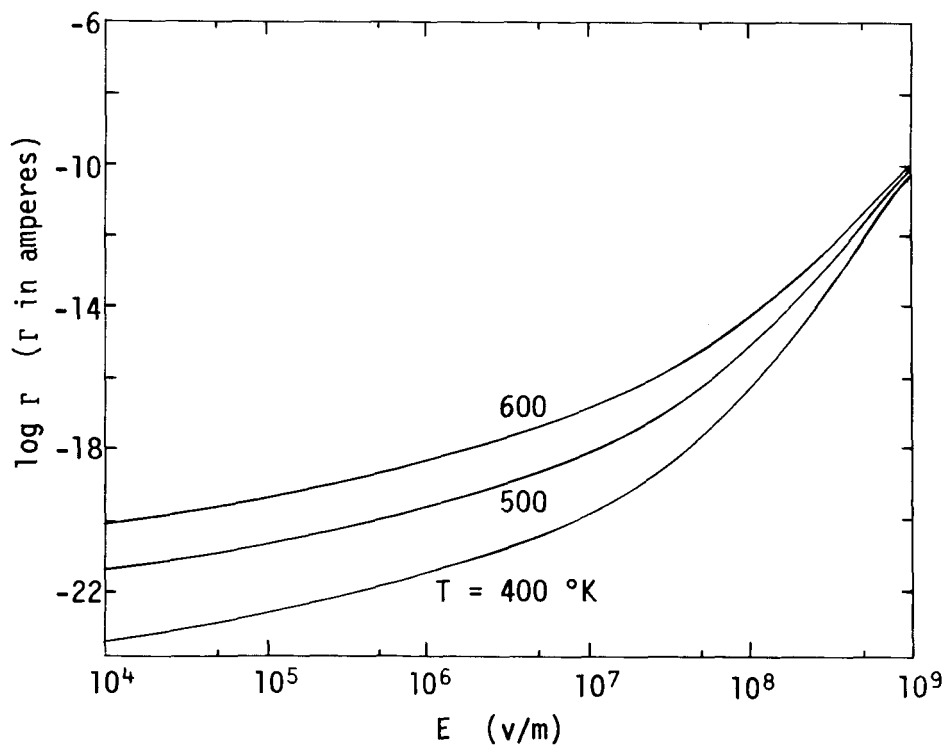


Fig.6. Plots of  $\Gamma$  as a function of  $E$  for various  $T$ .

By use of Eq.(7) for  $\sigma$ , it is possible to express the current density in terms of fundamental constants and pertinent parameters. Thus

$$\frac{j}{\sigma} = \Gamma = \frac{e}{2L} \left( \frac{\beta}{2\pi m} \right)^{\frac{1}{2}} \frac{e^{\beta\sqrt{aE}}}{(\pi B/\sqrt{8a})E^{-3/4} - \beta},$$

$$j = \sigma\Gamma = (\epsilon_0/e^2\lambda) \left( \mu + eEs - \frac{j}{Ae\sigma_0} \right) \Gamma, \quad (27)$$

whence

$$j = \frac{Ae\sigma_0(\mu + eEs)g\Gamma}{Ae\sigma_0 + g\Gamma}, \quad (28)$$

with  $g = \epsilon_0/e^2\lambda = 8.64 \times 10^{35} \text{ m}^{-2} \text{ joules}^{-1}$  for  $\lambda = 4\text{\AA}$  (Sec. II).

The parameters appearing in Eq.(28) are  $\mu = \phi + \epsilon_F - \epsilon_b - W_0''$ ,  $\sigma_0$ , and the temperature, which enters via  $\Gamma(E,T)$ . Since  $\Gamma$  is not available in analytic form, Eq.(28) is plotted in Figs. 7-13 for various values of the parameters. Because Eq.(28) is a three parameter family, a large number of plots would be required to give a relatively complete idea of its behavior; Figs. 7-13 have been chosen as exhibiting the salient features of this behavior.

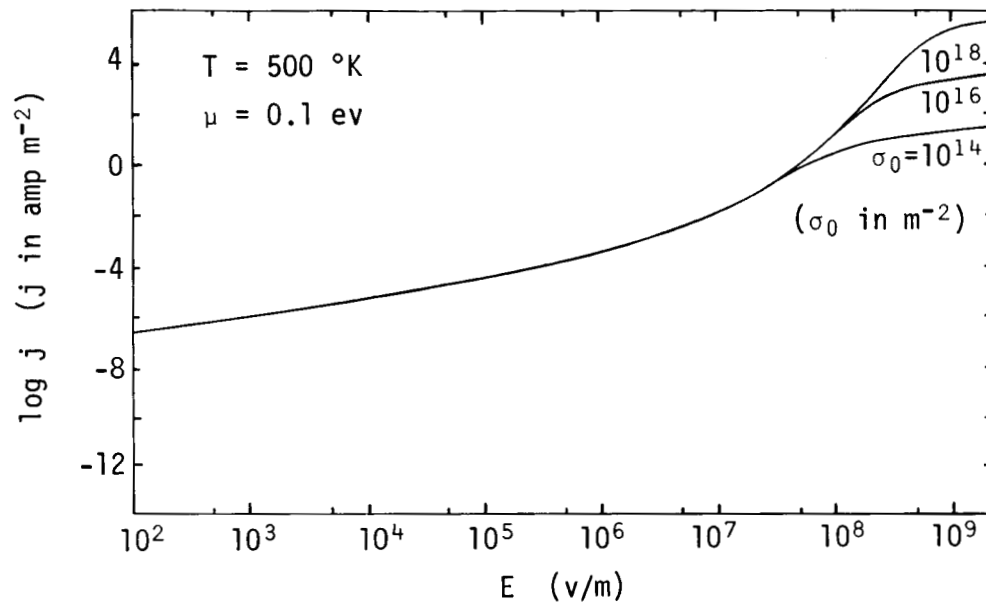
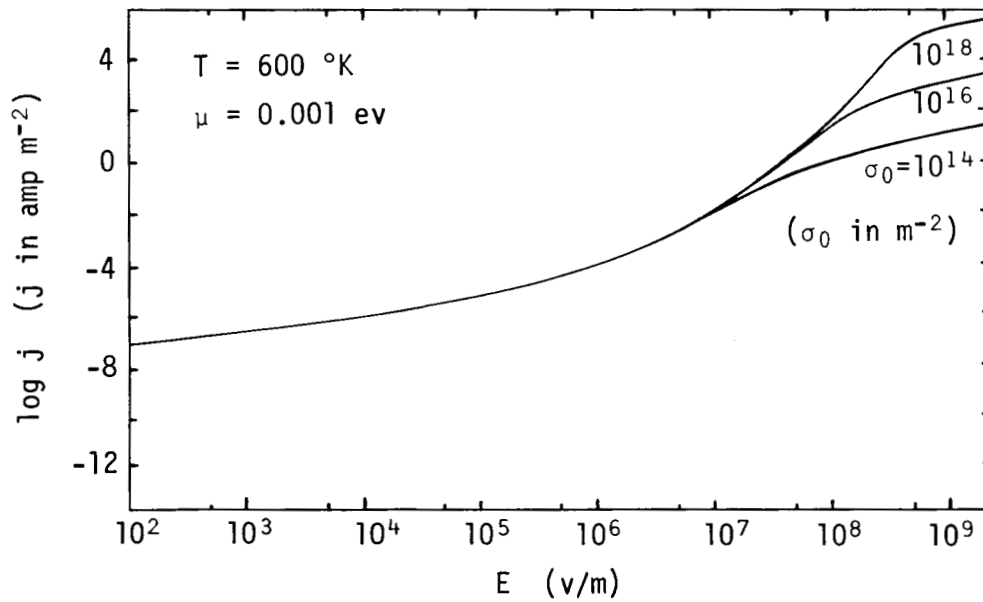
In explanation, Figs. 7 and 8 are typical of the effect on  $j$  of a variation in the adsorbed neutral atom density  $\sigma_0$ , per se. (The effect of  $\sigma_0$  on  $\mu$  will be discussed later). It can be seen that  $j$  is almost completely independent of  $\sigma_0$  for  $E \leq 2.25 \times 10^7 \text{ v/m}$ .

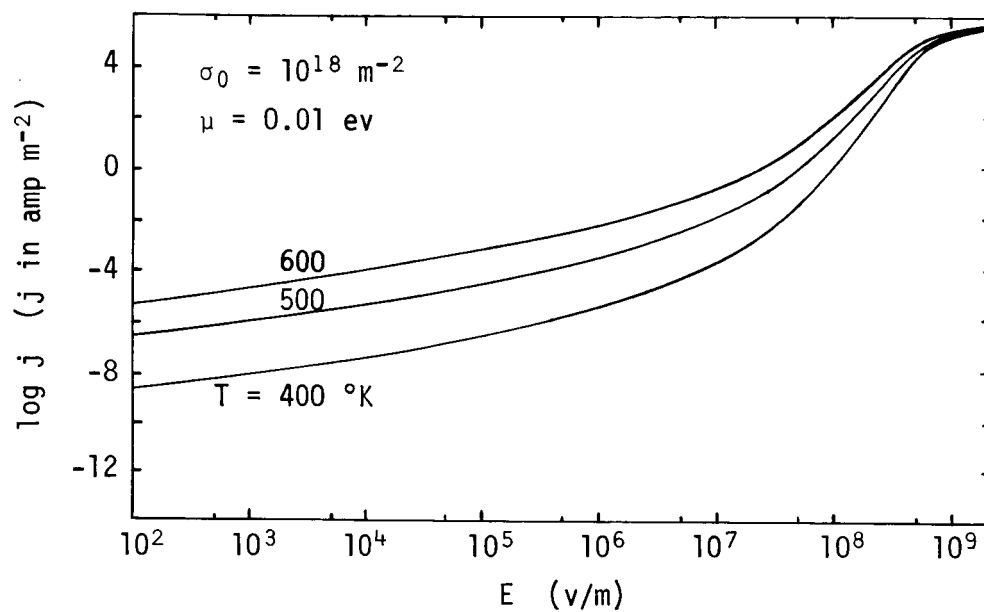
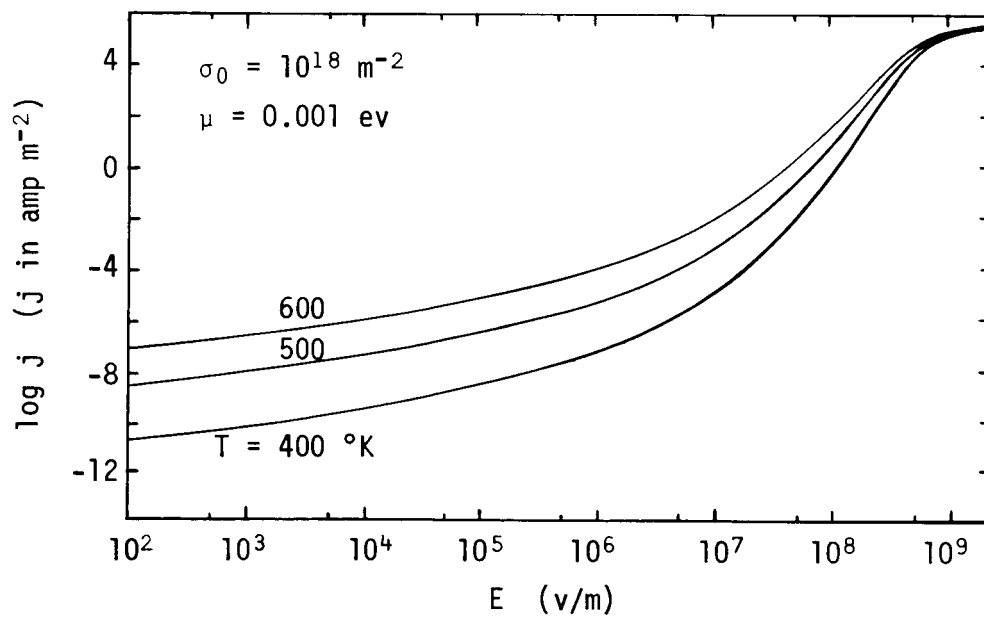
For fields  $E \geq 3 \times 10^8$  v/m, on the other hand,  $j$  becomes approximately a linear function of  $E$  and  $\sigma_0$ . That this is generally true, rather than peculiar to these two plots, can be seen from Eq.(28). Clearly, when  $g\Gamma \ll Ae\sigma_0$ ,  $j \approx (\mu + eEs)g\Gamma$  results, which is independent of  $\sigma_0$  (and of  $A$ ); this corresponds to the lower field range (see Fig.6 for  $\Gamma$ ). With  $\Gamma$  large enough so that  $g\Gamma \gg Ae\sigma_0$ ,  $j \approx Ae\sigma_0(\mu + eEs)$ , which is linear in  $E$  and  $\sigma_0$ . Note that since the transition rate constant  $A$  enters into Eq.(28) in exactly the same way as  $\sigma_0$ , the same remarks apply to  $A$  as to  $\sigma_0$ . Therefore, in the region  $g\Gamma \ll Ae\sigma_0$ , which is the most interesting for present purposes, an error in  $A$  of a few orders of magnitude will have no significant effect on  $j$ .

Next, Figs. 9 and 10 indicate the behavior of  $j$  with  $T$ . The value  $\sigma_0 = 10^{18} \text{ m}^{-2}$  was chosen as approximating real conditions. The very low values of  $\mu$  were used because in most cases,  $\mu \approx 0$  for a discharge (see Sec.VII).

Finally, Figs. 11, 12, and 13 show the dependence of  $j$  on  $\mu$  when  $\mu$  is small. The temperatures used are in the range of interest of most cesium discharges. The reason for considering  $\mu$  a parameter will be taken up in the next section.

It has been pointed out by Dr. H.S. Robertson that the above-found independence of  $j$  on the details of the ionization rate is, on physical grounds, not surprising. This is because the emission process is essentially a current flow through two series

Fig.7. Dependence of  $j$  on  $\sigma_0$ .Fig.8. Dependence of  $j$  on  $\sigma_0$ .

Fig.9. Dependence of  $j$  on  $T$  for  $\mu = 0.01$  eV.Fig.10. Dependence of  $j$  on  $T$  for  $\mu = 0.001$  eV.

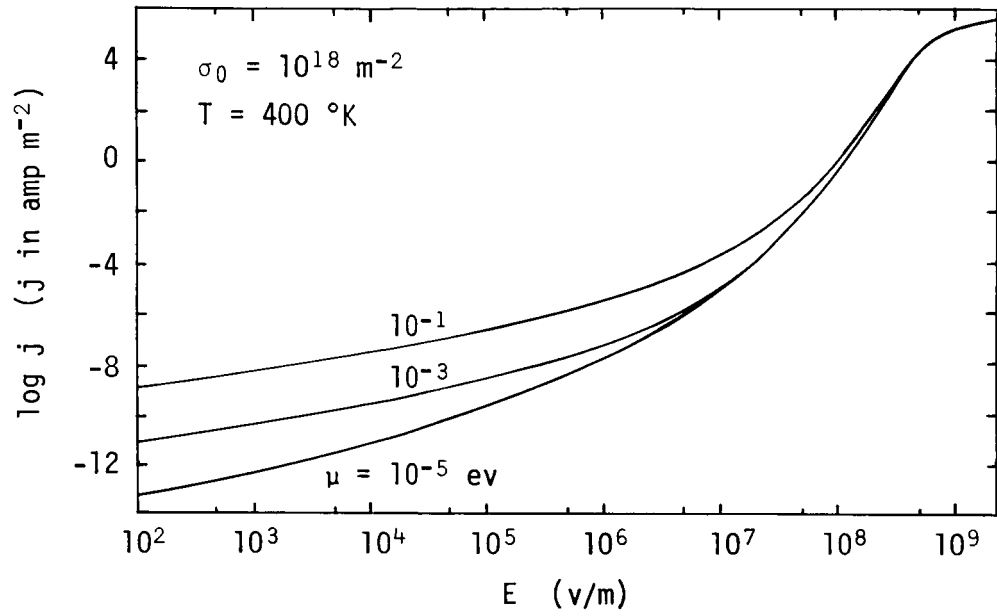


Fig.11. Dependence of  $j$  on  $\mu$  for  $T = 400 \text{ }^\circ\text{K}$ .

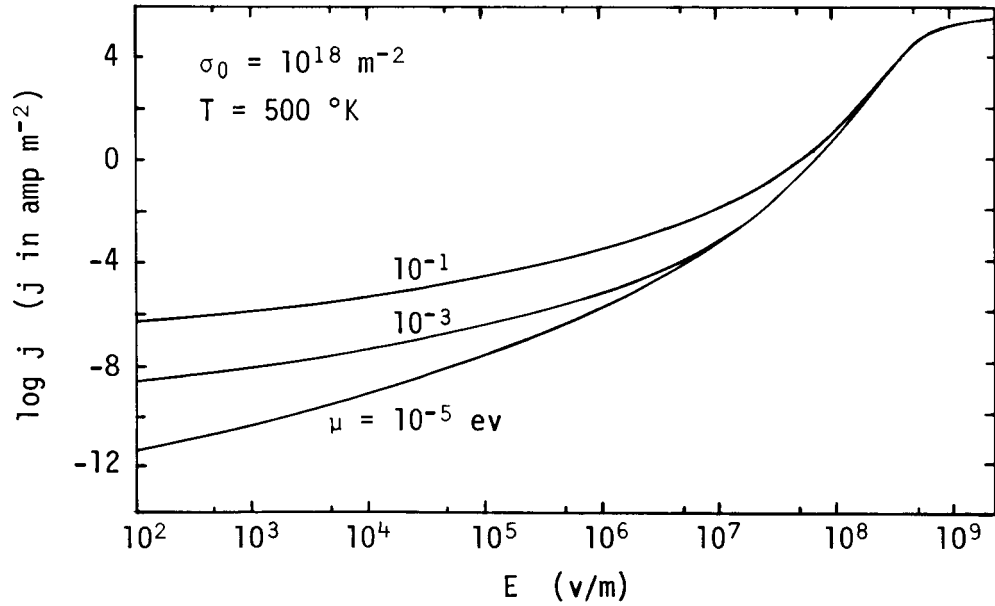


Fig.12. Dependence of  $j$  on  $\mu$  for  $T = 500 \text{ }^\circ\text{K}$ .

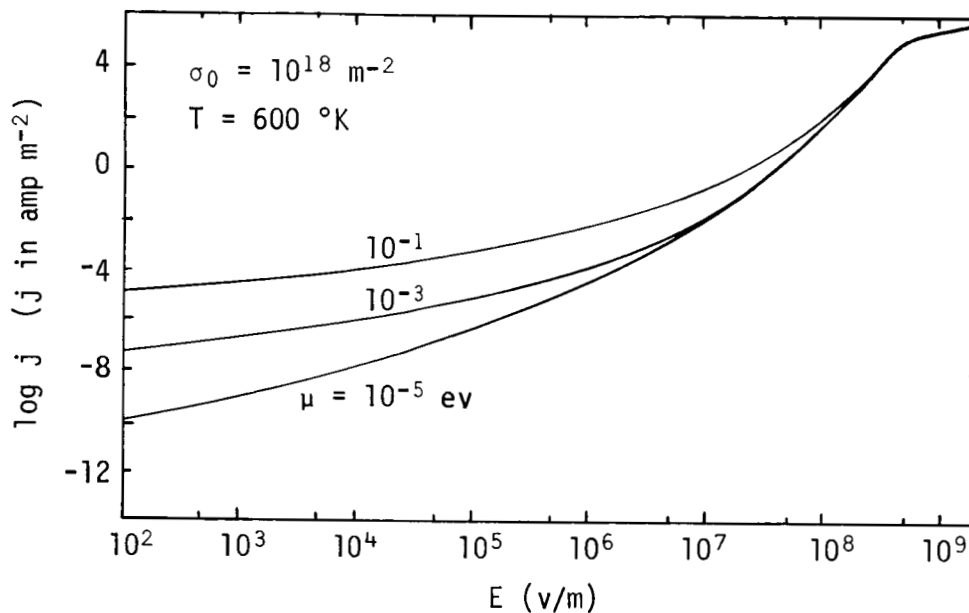


Fig.13. Dependence of  $j$  on  $\mu$  for  $T = 600 \text{ }^\circ\text{K}$ .

conductances, an "ionization rate conductance" and a "transmission conductance". For sufficiently high ionization rates, the ionization conductance, which is not accurately calculable at present, is ordinarily so large compared to the transmission conductance (which can be accurately calculated) that it can be considered a short circuit. Thus the result that the emission current, for small currents, is independent of the details of the ionization rate. This conclusion is independent of the functional form of  $w(\Delta\epsilon)$ , and so it lends support to the procedure leading to Eq.(28).

## VII. THE DEPENDENCE OF THE WORK FUNCTION ON THE ADSORPTION FRACTION

It will now be necessary to clarify why  $\mu$  has been chosen as a parameter, when it would seem to be a fixed quantity for given electrode and discharge medium combinations. In fact it is not; the findings of Taylor and Langmuir<sup>2,14</sup> have shown a strong dependence of the work function of tungsten on the degree of cesium coverage on the surface. If  $\phi$  depends on  $\sigma_0$ , then so will  $\mu = \phi + (\epsilon_F - \epsilon_b) - W_0^0$ . Thus  $\sigma_0$  actually enters Eq.(28) in two ways: directly as it appears there, and also through its effect on  $\mu$ . It has already been mentioned that in the current range of interest,  $\sigma_0$  has very little effect as it enters directly in  $j(E)$ . However, through its effect on  $\mu$ , it very strongly influences  $j(E)$ . This is borne out clearly by Figs. 11, 12, and 13.

The studies<sup>2,14</sup> of Taylor and Langmuir of cesium adsorption on tungsten have provided valuable information on the effect of adsorbed fractional monolayers of "neutral" atoms on the electron work function  $\phi$ . Theoretically, the adsorbed fractional layer is considered<sup>15</sup> as a polarizable dipole sheet which for electro-positive atoms such as cesium acts to reduce the work function from its value for a bare surface. For small fractional coverages ( $\leq 15\%$ ), the experimental results<sup>2</sup> give a linear decrease in work function as the fractional coverage is increased. A decrease in work function of 1 ev occurs at a coverage of -8.5%.



Because the dipole moment per adsorbed atom decreases with an increasing coverage (due to the depolarizing effect of the array), the work function decrease rate drops off. A maximum decrease of about 3 ev is found for a coverage of 67% monolayer. The value  $4.8 \times 10^{14} \text{ cm}^{-2}$  determined by Langmuir is taken as a monolayer for cesium on tungsten.

The explanation of the reduction in work function by a "polarizable layer" at the surface leaves a lingering dissatisfaction. Many objections can be raised about such a mechanism. In a review article on thermionic electron emission, Nottingham<sup>15</sup> points out the almost complete lack of theoretical understanding of such devices as the thoriated tungsten emitter, which depends on just such a reduction in work function for its efficiency. While this particular device has had uncounted applications over some four decades, it appears to be as well understood today as it was in the days of its discovery.

For present purposes, however, it suffices to say that the effect clearly exists. Furthermore, sufficient information is available so that its behavior can be known; this is all that is required here.

Considering these results of Taylor and Langmuir, it is clear that the quantity  $\mu$  might become zero or even negative. For a bare tungsten surface,  $\phi = 4.6 \text{ ev}$ . The value of  $W_0''$ , the perturbed valence level due to all the sources indicated in Secs. II

and III, has not been calculated; however, the value 3.6 ev arrived at by Gadzuk<sup>3</sup> by considering only surface and image forces is probably reliable, since these are the most powerful at close range. Additional evidence that  $\mu \approx 1$  ev for a bare tungsten surface is provided by Rasor and Warner<sup>16</sup>, who obtain a value of about 1.05 ev through a consideration of the known adsorption and vaporization energies of cesium, rather than by a quantum mechanical calculation of the level shift. Levine<sup>17</sup> also obtains the value 1.05 ev. Thus  $\mu \approx 1$  ev for a bare surface will be used, while with only 8.5% monolayer,  $\mu \approx 0$ . These results will be considered in Sec. VIII.

In the event that  $\mu$  becomes negative, the emission current remains zero until a value of  $E$  is reached at the anode surface such that (see Eq.(28))  $\mu + eEs > 0$ , at which point emission will commence. That is, no emission would be possible with  $\mu + eEs \leq 0$  because no ionization would be taking place on the anode surface.

Under ordinary conditions, it is easy to infer from known data<sup>2,14,16</sup> that most of the anode will be operating in the region around  $\mu = 0$ . However, irregularities in surface properties can cause significant variations in  $\mu$  over the surface. The consequences of this variation will be indicated in Sec.VIII.

## VIII. DISCUSSION OF THE EMISSION EQUATION

The result (28) for the ion emission current is directly applicable to the cesium vapor discharge. However, it is first necessary to relate the ion current to the total discharge current, since no method presently exists by which the ion current alone can be measured. The ion current at the anode, as well as at other points in the discharge, is ordinarily only a small fraction of the total current; the major portion is due to electron flow. In a recent study, Robertson<sup>18</sup> obtains a result that gives the ratio of the ion current density at the anode surface to that in the plasma adjoining the anode. Since the ratio of electron to ion current density in the plasma is simply the ratio of the respective mobilities, it is possible to infer the ratio of ion to total current both in the plasma and at the anode surface. Thus the expression (28) can be related to the experimentally measurable discharge current.

As a convenient guide, the discharge may be considered as consisting essentially of a bundle of contiguous filamentary current elements originating at one electrode and terminating at the other. While currents to the walls by means of ambipolar diffusion will certainly occur, these do not essentially modify the picture. For fixed discharge parameters (discharge medium, pressure, temperature, confining geometry, etc.) the discharge

dynamics are essentially determined by the external circuit conditions; the discharge operates at a given set of conditions in accommodation to the demands of the external circuitry. That is, all internal plasma activity, such as ionization and loss rates, charged and neutral currents, and so on, must adjust to meet externally imposed conditions. The situation is too complicated to describe in detail; moreover, much of it is not yet fully understood. For a fairly up-to-date discussion, some excellent review articles in the "Handbuch der Physik" are available<sup>19</sup>. A number of texts<sup>20-23</sup> can also be consulted.

Equation (28), in combination with the results obtained in reference 18, can be utilized to give the particular accommodation that must occur at the anode surface for steady state. That is, the electric field that must develop at the anode for a given total current may be determined. Physically, this means that the charge distributions in the anode vicinity will arrange themselves such that the required field results. Because of the dependence of Eq.(28) on  $\mu = \phi - W_0''$ , it can immediately be foreseen that difficulties will develop in obtaining a description of anode conditions, since a real anode is not at all a structureless continuum, but exhibits variations in work function and adsorption properties. Since these properties determine  $\mu$ , and hence  $j$ , it is clear that a uniform description of anode fields is not possible. That is, the microproperties of a particular

anode will be all-important in determining the conditions at its surface. The situation is not unlike that of electron field emission, where the verification of the Fowler-Nordheim equation was for many years impeded by just such variations in surface properties. Among the many anode surface irregularities which can occur may be mentioned substrate imperfections, surface contamination, oxide flakes, gross physical features due to fabrication, and so on.

It thus becomes necessary, in terms of the above picture of the discharge as a bundle of current elements, to individually consider the elements of area which are the positive (anode) termini of these current elements. The emission from these elements of area will then proceed according to Eq.(28) as particularized by the local value of  $\mu$ . The value of  $\mu$  may be obtained from the data of reference 2, provided the anode microproperties are known. The much more recent study of Rasor and Warner<sup>16</sup> is probably more useful in that it gives the reduction in work function for a variety of electrode-discharge medium combinations.

As a final point, mention may be made of an experimental finding of Langmuir and Kingdon<sup>24</sup> on the emission of cesium ions with an applied field. They obtained the result that ion emission in the presence of an adsorbed fraction  $\theta$  is negligible except when  $\theta$  is very small. The fields used by them were in the

lower field range of Figs. 11-13. The very rapid drop-off in current as  $\mu$  decreases ( $\theta$  increases) with fixed field is there clearly evident, so that in this detail, Eq.(28) agrees qualitatively with experiment.

In summary, it is necessary to point out that because of the approximations and assumptions leading to the emission equation, the present investigation is in a sense an exploratory one. In some cases, such as the assumptions on the ion potential energy near the anode surface and the representation for the surface ionization rate, the procedures used have been an unavoidable necessity; sufficient information is not at present available to permit definite statements to be made. Other assumptions, e.g., the utilization of a constant mean distance  $\ell$  of the ions from the anode surface, were made for the sake of convenience; it was not felt worthwhile to introduce the considerable complication of including the field dependence of  $\ell$  since, under ordinary conditions, most of the ions are clustered around  $x = 4-6 \text{ \AA}$ .

While many of the elements incorporated into Eq.(28) are thus open to refinement and improvement as more becomes known about them, it is felt that the process underlying the calculation, i.e., the steady-state surface ion supply derived in Sec.III, is basically sound, and as such constitutes a reliable foundation for the construction of the emission equation.

## APPENDIX

It was not found possible to integrate Eq.(19) with  $T(W)$  as given by Eqs. (14), (17) and (18). In this section an approximation to  $T(W)$  will be found by means of which the integration can be effected.

The expression to be approximated is

$$T(y) = 1/[1 + \exp\{Q(y)\}] = 1/[1 + \exp\{\alpha y^{-3/2}v(y)\}], \quad (29)$$

where  $v(y)$  is given in Eqs. (18) and  $y = W_m/W$ . When the approximating expression found here for  $T(y)$  is put in Eq.(19) and the integral evaluated, it is found that the total contribution from  $Q(y) \geq 30$  is completely negligible. Therefore, for the sake of brevity, the discussion will be limited to  $0 \leq Q(y) \leq 60$ . Since  $Q(y) = \alpha(E)y^{-3/2}v(y)$ , and  $\alpha(E)$  is very large under all conditions ( $\alpha \geq 3.61 \times 10^3$ ),  $v(y) \approx 0$  will be required if  $0 \leq Q \leq 60$  is to be satisfied; i.e., it is necessary that  $y \approx 1$  (see Fig.14 for  $v(y)$ ).

Suppose now that a function  $U(y)$  can be found such that

$$\left. \begin{aligned} U(y) &\approx v(y) \text{ for } v(y) \approx 1, \\ U(1) &= v(1), \\ U'(1) &= v'(1), \end{aligned} \right\} (30)$$

where the prime denotes differentiation with respect to  $y$ , and

furthermore such that  $[U(y) - v(y)]/v(y) \rightarrow 0$  monotonically as  $y$  approaches 1. Then the worst possible case to consider in the approximation process is that for which  $\alpha(E)$  in Eq.(29) takes on its minimum value, since this will result in the largest departure from  $y = 1$  which will satisfy  $Q(y) = \alpha y^{-3/2} v(y) \leq 60$ . That is, larger values of  $\alpha(E)$  will require values of  $y$  closer to  $y = 1$  in order to retain  $Q \leq 60$ , and this will increase the accuracy of the approximation by virtue of the fact that  $(U - v)/v \rightarrow 0$  monotonically as  $y \rightarrow 1$ .

The smallest value of  $\alpha = BE^{-3/4}$  of relevance to a tunnelling process is  $\alpha_m = 3.61 \times 10^3$  (the field for which the barrier collapses is  $2.25 \times 10^9$  v/m). Therefore, the search for an approximation will be confined to this minimum value of  $\alpha$ ; if a good approximation for this case can be found, then it will be even better as the field is increased.

As a convenient outline, the following will be done. The interval  $0 \leq y \leq 1$  is divided into three regions  $R_1, R_2, R_3$ , (see Sec.VI), such that  $R_1: 0.995 \leq y \leq 1$ ;  $R_2: 0.990 \leq y \leq 0.995$ ;  $R_3: 0 \leq y \leq 0.990$ . The result is then obtained that the emission over the three regions is such that  $j_2 < 10^{-8} j_1$ , while  $j_3 \approx 10^2 j_2$  at the very most. Therefore, if it can be shown that the approximating expression is valid in both  $R_1$  and  $R_2$ , then only the contribution from  $R_1$  need be retained. For the contribution from  $R_2$  is then validly approximated but negligible,



while that from  $R_3$  is at most a relatively small multiple of that from  $R_2$ . A simple expression that has been found to satisfy the conditions (30), as well as the monotonicity requirement, is

$$U(y) = (\pi/\sqrt{8})(1 - y^{3/2}). \quad (31)$$

The factor  $\pi/\sqrt{8}$  arises in fitting  $U'(1) = v'(1) = -3\pi\sqrt{2}/8$ .

The following must be shown: (1)  $[U(y) - v(y)]/v(y) \rightarrow 0$  monotonically as  $y \rightarrow 1$ , and (2) in  $R_1$  and  $R_2$ , the expression  $\tau(y) = [1 + \exp\{\alpha y^{-3/2}U(y)\}]^{-1}$  is a good approximation to  $T(y) = [1 + \exp\{\alpha y^{-3/2}v(y)\}]^{-1}$ . The relative error in  $Q$  due to the replacement  $v(y) \rightarrow U(y)$  is  $\Delta Q/Q = \alpha y^{-3/2}[U(y) - v(y)]/\alpha y^{-3/2}v(y) = (U - v)/v$ . Therefore, if  $(U - v)/v \rightarrow 0$  monotonically as  $y \rightarrow 1$ , so does  $\Delta Q/Q$ .

It is straightforward but tedious algebra to show rigorously that  $U/v \rightarrow 1_+$  as  $y \rightarrow 1_-$ . In order to cover the range of interest ( $Q \leq 60$ ) to the necessary accuracy, eight terms were required in the series expansions for the elliptic integrals  $F(k)$ ,  $K(k)$  appearing in  $v(y)$ . This will not be reproduced here; for  $y$  very close to 1, three terms in the series for  $F(k)$ ,  $K(k)$  give sufficient accuracy. The result is  $v(y) \approx 3\pi(1 - y^2)/8\sqrt{2}$ , so that

$$\Delta Q/Q = \frac{U}{v} - 1 \approx \frac{4}{3} \frac{1 - y^{3/2}}{1 - y^2} - 1. \quad (32)$$

Since both  $1 - y^{3/2}$ ,  $1 - y^2$  approach zero as  $y \rightarrow 1$ , they may be replaced by their derivatives according to l'Hospital's rule:

$$\Delta Q/Q = \sqrt{y}/y - 1 = 1/\sqrt{y} - 1,$$

which clearly approaches zero monotonically from above as  $y \rightarrow 1$  from below. Table I and Fig.14 show this behavior clearly.

Next, the relative error  $[\tau(y) - T(y)]/T(y)$  over  $R_1$  and  $R_2$  will be found, or rather at the end-points. The relative error within the intervals will be smaller than at the end-points by virtue of the monotonicity of  $\Delta Q/Q$ .

The values of  $Q$  at  $y = 0.995, 0.990$  can be obtained from the computed values of  $v(y)$  in Table I, and by using  $\alpha_m = 3.61 \times 10^3$ . These are found to be  $Q \approx 30, 60$ , respectively. Therefore, for either of these end-points,  $T \approx \exp(-Q)$  to very high accuracy. Whereupon, if there is an error  $\Delta Q$  in  $Q$  due to the replacement  $v(y) \rightarrow U(y)$ , then the error in  $T$  is

$$\Delta T = \sum_{n=1}^{\infty} \frac{1}{n!} T^{(n)}(Q) (\Delta Q)^n, \quad (33)$$

where  $T^{(n)} = \frac{d^n}{dQ^n} T(Q) = (-1)^n T$ . Hence

$$\Delta T = T \sum \frac{(-1)^n}{n!} (\Delta Q)^n = T[\exp(-\Delta Q) - 1],$$

and the relative error in  $T$  is

$$\Delta T/T = e^{-\Delta Q} - 1. \quad (34)$$

The values of  $\Delta Q = \alpha_m y^{-3/2}(U - v)$  for  $y = 0.995, 0.990$  can be

obtained by utilizing Table I; there results  $\Delta Q(0.995) = 0.00945$ ,  $\Delta Q(0.990) = 0.0385$ . Hence Eq.(34) gives  $(\Delta T/T)_{0.995} = -0.009$ ,  $(\Delta T/T)_{0.990} = -0.037$  as the relative errors in T over  $R_1, R_2$ , respectively. Thus the replacement  $v(y) \rightarrow U(y)$  is valid over  $R_1, R_2$ .

Table I. Comparison of  $v(y)$  and  $U(y)$ , together with the relative error  $\delta(y) = [U(y) - v(y)]/v(y)$ .

$y$	$v(y)$	$U(y)$	$\delta(y)$
0.00	1.0000	1.1107	0.111
0.10	0.9817	1.0755	0.096
0.20	0.9370	1.0115	0.080
0.30	0.8718	0.9282	0.065
0.40	0.7888	0.8300	0.052
0.50	0.6900	0.7174	0.040
0.60	0.5768	0.5945	0.031
0.70	0.4504	0.4603	0.022
0.80	0.3117	0.3154	0.014
0.90	0.1613	0.1625	0.007
0.95	0.0820	0.0823	0.003
0.990	0.0166 086	0.0166 191	0.0006
0.995	0.0083 173	0.0083 199	0.0003
1.000	0	0	0

It was stated earlier in this section that the contribution to the integral (19) over  $R_3$  is at most about  $10^2 j(R_2)$ . That such is the case can be easily seen by rewriting (19) entirely in terms of  $y = W_m/W$  and making the replacement  $W_0 \rightarrow -\infty$  (note that this replacement will increase the contribution from  $R_3$ , yet it remains completely negligible). Equation (19) therefore

becomes

$$j = H(\sigma, \beta, L, W_m) \int_0^1 \frac{e^{-\beta W_m/y}}{1 + \exp[\alpha y^{-3/2} v(y)]} \frac{dy}{y} \quad (35)$$

Thus even if the integrand in (35) were constant over  $R_3$ , the contribution therefrom would be  $j(R_3) \leq (0.990/0.005) \times j(R_2) \approx 200j(R_2)$ . In reality, the integrand decreases rapidly as  $y \rightarrow 0$ .

In view of the above,  $Q$  and  $T$  are reliably approximated by the expressions

$$Q(y) \approx \alpha y^{-3/2} (\pi/\sqrt{8}) (1 - y^{3/2}) = \gamma (y^{-3/2} - 1), \quad (36)$$

$$T(y) \approx \tau(y) = [1 + \exp\{\gamma (y^{-3/2} - 1)\}]^{-1}, \quad (37)$$

with  $\gamma(E) = \pi\alpha(E)/\sqrt{8}$ .

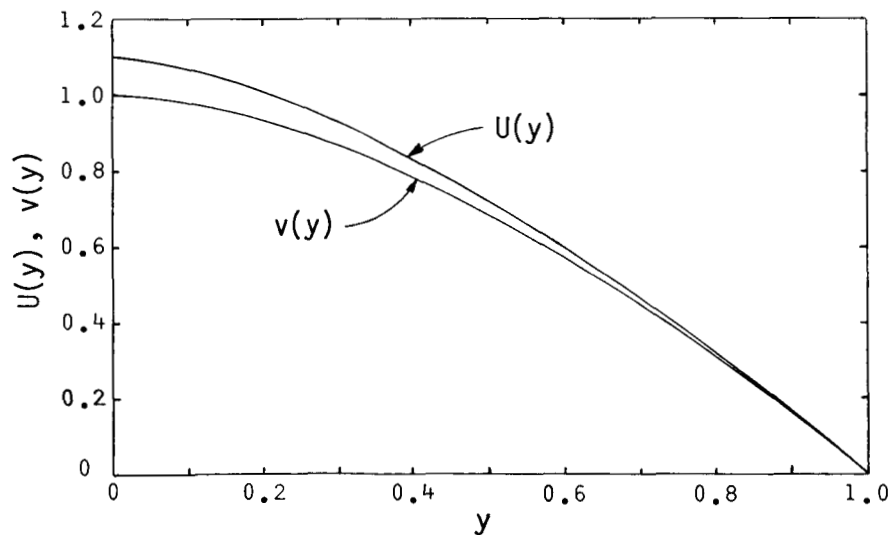


Fig.14. Plots of  $v(y)$  and  $U(y)$ .

A difficulty that remains is that if Eq.(37) is put in the emission equation (19), it turns out to be still impossible to perform the integration. Therefore,  $\tau(y)$  must itself be approximated by some expression that will retain a reasonable accuracy, while at the same time permitting integration of Eq.(19).

It may seem that an unnecessary detour was taken in arriving first at  $\tau(y)$ , which must then be also approximated. However, it will be seen shortly that  $\tau(y)$  is approximated by an expression  $\theta(y)$  of rather different form. Had  $\theta(y)$  been used to compare directly with  $T(y)$ , it would have been difficult to say anything about the error propagation. This is because the exponent in  $T(y)$  is parametric in  $\alpha$ , and since the fit must be made by considering the total expression for the exponent, it becomes necessary to obtain the value of  $y$  as  $y(\alpha)$  for a given value of the exponent. This is an impossibly tedious task if the original expression  $\alpha y^{-3/2} v(y) = n$ , say, is considered, whereas it is a simple matter to invert  $\gamma(y^{-3/2} - 1) = n$  for  $y = y(\gamma, n)$ .

Consider now Eq.(37) for  $\tau(y)$ . The range of  $\tau(y)$  is seen to be  $0 \leq \tau(y) \leq 1/2$ , corresponding to  $0 \leq y \leq 1$ . From here on, it will be easier to work in terms of  $x = 1/y = W/W_m$ , the reason for having so far used  $y$  as variable being that it made the expressions (18) much simpler to work with. Thus Eq.(37) becomes

$$\tau(x) = [1 + \exp\{\gamma(x^{3/2} - 1)\}]^{-1}, \quad (38)$$

with

$$\left. \begin{array}{l} 0 \leq \tau(x) \leq 1/2, \\ \text{for} \\ \infty \geq x \geq 1. \end{array} \right\} (39)$$

The behavior of  $\tau(x)$  is as shown in Fig.15, wherein the dashed part of the curve corresponds to energies above the barrier. This is not considered here.

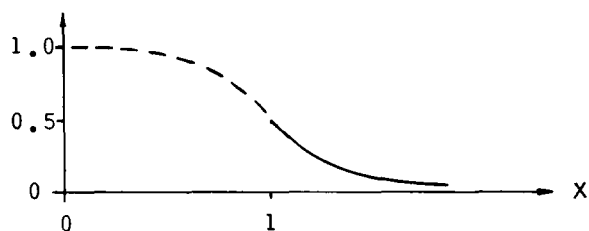


Fig.15. Behavior of  $\tau(x)$ .

From the form of  $\tau(x)$ , together with the values at the end-points, the following suggests itself as a likely (and integrable) approximation:

$$\theta(x) = (1/2)e^{-c\gamma(x-1)} \approx \tau(x), \quad (40)$$

where  $c$  must be fitted. It is clear that the end-point values of  $\theta(x)$ ,  $\tau(x)$  are identical for any nonzero value of  $c$ .

The values of  $\theta(x)$  and  $\tau(x)$  can now be easily compared because of the simple analytic forms of the exponents in each. It will only be necessary to compare for values of the exponent in

Eq.(38) which lie in  $0 \leq \gamma(x^{3/2} - 1) \leq 60$ . Outside this range,  $\theta(x) > T(x)$ , so that the contribution to  $j$  over  $60 \leq (\exp) \leq \infty$  will be increased by the approximation  $\theta(x) \approx T(x)$ , yet is completely negligible (see Sec.VI). Hence the actual contribution if  $T(x)$  were used would certainly be negligible over this latter interval.

Suppose then that  $\gamma(x^{3/2} - 1) = \eta \leq 60$ ; this can be inverted to give  $x = (1 + \eta/\gamma)^{2/3} \approx 1 + 2\eta/3\gamma$ , because  $\gamma \approx 4000$ . Therefore,  $\gamma(x - 1) \approx 2\eta/3$ . The choice  $c = 1$  in Eq.(40) gives a good fit; hence the expressions

$$\begin{aligned}\theta(\eta) &= (1/2)\exp(-2\eta/3), \\ \tau(\eta) &= (1 + e^\eta)^{-1}\end{aligned}\tag{41}$$

will be compared. Values of  $\theta(\eta)$  and  $\tau(\eta)$  over  $0 \leq \eta \leq 60$  are given in Table II, together with the weighted relative error  $\delta = \Omega(\eta)(\theta - \tau)/\tau$ . The weighting factor  $\Omega(\eta)$  is just the value of the integrand of Eq.(19) normalized so that  $\Omega(1) = 1$ ; that is,  $\Omega(1) = 1 = b(1/2)\exp(-\beta W_m)$ , so that  $b = 2\exp(\beta W_m)$ . Therefore,  $\delta = 2(\theta - \tau)\exp[-\beta W_m(x-1)]$ . For  $0 \leq \eta \leq 60$ ,  $x-1 \approx 2\eta/3\gamma$ , and using  $W_m$  for  $E = E_m = 2.25 \times 10^9$  v/m (i.e.,  $-W_m$  has its maximum value for this field), one can obtain  $0 \leq [-\beta W_m(x-1)] \leq 0.0206$ . Hence, for comparison purposes in this range,  $\exp[-\beta W_m(x-1)] \approx 1$ , and  $\delta \approx 2(\theta - \tau)$  can be used.

In view of the fact that the weighted error (see Table II)

resulting from the substitution  $\tau(x) \rightarrow \theta(x)$  is everywhere within about 2%,  $\theta(x)$  will be considered a fair representation for  $\tau(x)$  and  $T(x)$ . Therefore,

$$T(W) \approx \tau(W) \approx \theta(W) = (1/2)\exp[-\gamma(W/W_m - 1)], \quad (41)$$

where, as previously stated,  $W$  ranges over  $W_0 \leq W \leq W_m$ .

Table II. Comparison of  $\theta(n)$  and  $\tau(n)$ , together with the weighted relative error  $\delta(n) = 2[\theta(n) - \tau(n)]$ .

$n$	$\tau(n)$	$\theta(n)$	$\delta(n)$
0	0.5000	0.5000	0
0.01	0.4975	0.4970	-0.0005
0.02	0.4950	0.4935	-0.0015
0.03	0.4925	0.4900	-0.0025
0.05	0.4870	0.4835	-0.0035
0.10	0.4750	0.4675	-0.0075
0.20	0.4500	0.4375	-0.0125
0.50	0.3775	0.3580	-0.0195
1.00	0.2680	0.2567	-0.0113
1.50	0.1825	0.1843	+0.0018
2.00	0.1180	0.1315	0.0135
3.00	0.0470	0.0675	0.0205
4.00	0.0175	0.0340	0.0165
5.00	0.0065	0.0175	0.0110
6.00	0.0025	0.0080	0.0055
10.00	$\sim \exp(-10)$	$\exp(-7.26)$	0.0010
15.00	$\sim \exp(-15)$	$\exp(-10.69)$	$\sim \exp(-10.69)$
20.00	.....	.....	.....
30.00	.....	.....	.....
45.00	.....	.....	.....
60.00	$\exp(-60)$	$\exp(-40.69)$	$\exp(-40.69)$



## LITERATURE CITED

1. R. H. Good, Jr., and E. W. Müller, Field Emission Article in Handbuch der Physik, Vol. 21, Springer-Verlag (1956).
2. J. B. Taylor and I. Langmuir, Phys. Rev. 44, 423(1933).
3. J. W. Gadzuk, Surf. Sci. 6, 133(1967).
4. D. S. Boudreaux and P. H. Cutler, Phys. Rev. 149, 170(1966).
5. D. S. Boudreaux and P. H. Cutler, Surf. Sci. 5, 230(1966).
6. J. W. Gadzuk, "Bonding Mechanism of Alkali-Metal Atoms Adsorbed on Metal Surfaces", NASA FAC. REPROD. N65-21038.
7. H. D. Hagstrum, Phys. Rev. 89, 244(1953).
8. H. D. Hagstrum, Phys. Rev. 91, 543(1953).
9. H. D. Hagstrum, Phys. Rev. 96, 325(1954).
10. H. D. Hagstrum, Phys. Rev. 96, 336(1954).
11. Hirschfelder, Curtiss and Bird, Molecular Theory of Gases and Liquids, John Wiley and Sons (1964).
12. S. C. Miller and R. H. Good, Jr., Phys. Rev. 91, 174(1953).
13. E. C. Kemble, The Fundamental Principles of Quantum Mechanics, Dover Publications (1958).
14. I. Langmuir, J. Amer. Chem. Soc., 54, 2798(1932).
15. W. B. Nottingham, Thermionic Electron Emission article in Handbuch der Physik, Vol. 21, Springer-Verlag (1956).
16. N. S. Razor and C. Warner, J. Appl. Phys. 35, 2589(1964).
17. J. D. Levine, Ph. D. Thesis, Dept. of Phys., M.I.T. (1963)
18. H. S. Robertson, Plasma Phys. Bull., 6 No.2, University of Miami (Aug., 1966).
19. Handbuch der Physik, Vols. 21 and 22, Springer-Verlag (1956).

20. S. Gartenhaus, Elements of Plasma Physics, Holt, Rinehart, and Winston (1964).
21. J. D. Cobine, Gaseous Conductors, Dover Publ. (1958).
22. W. B. Thompson, An Introduction to Plasma Physics, Addison-Wesley (1962).
23. C. L. Longmire, Elementary Plasma Physics, Wiley (1963)
24. I. Langmuir and K. H. Kingdon, *Science* 57, 58(1923); *Proc. Roy. Soc.* A107, 61(1925).